Output-Feedback Consensus Maneuvering of Uncertain MIMO Strict-Feedback Multiagent Systems Based on a High-Order Neural Observer

Yibo Zhang, *Member, IEEE*, Wentao Wu, *Graduate Student Member, IEEE*, Weixing Chen, Haibo Lu, and Weidong Zhang, *Senior Member, IEEE*

***Abstract*—In this article, a distributed output-feedback consensus maneuvering problem is investigated for a class of uncertain multiagent systems with multi-input and multi-output (MIMO) strict-feedback dynamics. The followers are subject to immeasurable states and external disturbances. A distributed neural observer-based adaptive control method is designed for consensus maneuvering of uncertain MIMO multiagent systems. The method is based on a modular structure, resulting in the separation of three modules: 1) a variable update law for the parameterized path; 2) a high-order neural observer; and 3) an output-feedback consensus maneuvering control law. The proposed distributed neural observer-based adaptive control method ensures that all followers agree on a common motion guided by a desired parameterized path, and the proposed method evades adopting the adaptive backstepping or dynamic surface control design by reformulating the dynamics of agents, thereby reducing the complexity of the control structure. Combined with the cascade system analysis and interconnection system analysis, the input-to-state stability of the consensus maneuvering closed loop is established in the Lyapunov sense. A simulation example is presented to demonstrate the performance of the proposed distributed neural observer-based adaptive control method for output-feedback consensus maneuvering.**

***Index Terms*—Consensus maneuvering, high-order neural observer, neural network adaptive control, output-feedback control, uncertain multi-input and multi-output (MIMO) multiagent systems.**

Manuscript received 23 March 2023; revised 8 July 2023 and 29 November 2023; accepted 23 December 2023. Date of publication 30 January 2024; date of current version 10 July 2024. This work was supported in part by the National Key Research and Development Program of China under Grant 2022ZD0119903; in part by the National Natural Science Foundation of China under Grant 52201369 and Grant U2141234; in part by the Shanghai Science and Technology Program under Grant 22015810300; in part by the Hainan Province Science and Technology Special Fund under Grant ZDYF2021GXJS041; in part by the China Post-Doctoral Science Foundation under Grant 2022M722053; and in part by the Oceanic Interdisciplinary Program of Shanghai Jiao Tong University under Grant SL2022PT112. This article was recommended by Associate Editor Q. Meng. *(Corresponding author: Weidong Zhang.)*

Yibo Zhang, Wentao Wu, and Weidong Zhang are with the Department of Automation, Shanghai Jiao Tong University, Shanghai 200240, China (e-mail: zhang297@sjtu.edu.cn; wentao-wu@sjtu.edu.cn; wdzhang@sjtu.edu.cn).

Weixing Chen is with the State Key Laboratory of Mechanical System and Vibration, School of Mechanical Engineering, Shanghai Jiao Tong University, Shanghai 200240, China (e-mail: wxchen@sjtu.edu.cn).

Haibo Lu is with the Robotics Research Center, Peng Cheng Laboratory, Shenzhen 518055, China (e-mail: luhb@pcl.ac.cn).

Color versions of one or more figures in this article are available at https://doi.org/10.1109/TCYB.2024.3351476.

Digital Object Identifier 10.1109/TCYB.2024.3351476

I. Introduction

In recent years, distributed cooperative control of multiagent systems has garnered significant attention due to its widespread application in various fields, such as unmanned marine vehicles, smart grids, and bionic robots [1], [2], [3]. Consensus, as one of the key topics in distributed cooperative control, has been a focal point, with numerous reported results, including leaderless consensus [4], [5], [6] and leader-following consensus [7], [8], [9], [10], [11], [12], [13], [14], [15], [16], [17]. In particular, leader-following consensus implies that followers reach an agreement on a common motion guided by a single leader [7], [8], [9], [10], [11], [12], [13], [14], [15], [16], [17]. In [7], a distributed adaptive leader-following consensus protocol is developed for linear agents with respect to a leader with a zero input. In [8] and [9], output sign-consensus is investigated for heterogeneous linear multiple agents under fixed and switching signed graphs. In [10], an asynchronous edge-based event-triggered mechanism is proposed for leader-following consensus. In [11], a distributed asynchronous sampled-data-based consensus control law is designed for a class of general linear multiagent systems. In [12], a secure consensus problem is studied for linear multiagent systems under event-triggered control subject to a sequential scaling attack. The above works in [7], [8], [9], [10], [11], and [12] focus on linear systems and naturally extend to nonlinear systems [13], [14], [15], [16], [17]. In [13], an optimal consensus problem is investigated for nonlinear systems subject to minimum-phase uncertain dynamics, unity-relative degree, and external disturbances. In [14], a distributed consensus problem is addressed for heterogeneous nonlinear systems under the switching topology, and a distributed dynamic compensator is designed to tackle internal uncertainties and external disturbances. In [15], distributed quantized adaptive consensus controllers are constructed using a command-filtered-backstepping method and state quantizers. In [16], fixed-time consensus control is studied for two classes of heterogeneous nonlinear multiagent systems. In [17], a neural adaptive leader-following consensus controller is developed for nonlinear multiagent systems, and a novel state transformation function is constructed to transform the constrained output into an equivalent unconstrained variable. Generally, leader-following consensus control considered in [7], [8], [9], [10], [11], [12], [13], [14], [15], [16], and [17]

can be categorized as consensus tracking along a time-dependent reference trajectory, where the control structure is spatial–temporal coupling. In certain applications, followers are directed along a parameterized path, where the spatial objective and the temporal objective need to be specified separately [18], [19], [20], such as cooperative surrounding of marine vehicles and cooperative search of mobile robots.

Maneuvering control has been formulated as a viable solution for spatial–temporal decoupling applications [20]. It comprises two tasks. The primary task is to drive an object to converge to a specified path parameterized by a scalar variable, commonly referred to as the path variable. The secondary task is to ensure that the object satisfies a given dynamic specification throughout the motion process associated with the primary task. When the path variable is predetermined for all future times, tracking control can be considered as a specific instance of maneuvering control [18]. Many maneuvering control methods have been reported, encompassing general linear systems [18], [19], uncertain nonlinear systems [20], [21], [22], and find natural extensions to various industrial applications, such as holonomic mobile robots [23], autonomous surface vehicles (ASVs) [24], [25], [26], [27], [28], unmanned underwater vehicles [29], and unmanned aerial vehicles [30]. It is noteworthy that the maneuvering control methods proposed in [18], [19], [20], [21], [22], [23], [24], [25], [26], [27], [28], [29], and [30] require access to the full-state information.

The acquisition of full-state information is challenging in real-world applications [31], [32], [33], [34]. It is rewarding to investigate the distributed cooperative control problem of nonlinear multiagent systems based on the output-feedback design [35], [36], [37], [38], [39]. In [35], distributed neural network adaptive controllers with fault tolerance capabilities are designed for nonstrict-feedback systems subject to intermittent actuator faults. In [36], an adaptive fuzzy tracking controller is developed for output-feedback leader-following consensus of nonlinear multiagent systems with the prescribed performance. In [37] and [38], observer-based fuzzy adaptive cooperative control methods are proposed using the backstepping design approach along with the command filters, employing the time-triggered [37] and event-triggered communication [38] separately. In [39], the distributed flocking problem is investigated for multiple ASVs without velocity sensors, using a data-driven extend state observer. The output-feedback control methods in [35], [36], [37], [38], and [39] are structured with the backstepping-like architecture, incorporating the adaptive backstepping or dynamic surface control design. However, this architecture increases the complexity of the control structure, thereby limiting its practical applications.

Building upon the preceding discussions, we delve into a distributed consensus maneuvering problem guided by a parameterized path under the directed topology herein. Consensus maneuvering is suitable for many practical scenarios. For instance, the formation of multiple ASVs can execute the search effort. Only a select number of vehicles are permitted to access the preplanned route during searching and need to perform a maneuvering task. Other vehicles receive the information from their neighbor vehicles and need to perform a tracking task. In this task scenario, the utilization of consensus maneuvering is deemed appropriate. A distributed neural observer-based adaptive control method is designed for consensus maneuvering of uncertain multi-input and multi-output (MIMO) strict-feedback multiagent systems subject to immeasurable states, uncertain nonlinearities, and external disturbances. The control method is proposed by using a modular design approach, resulting in the decoupling of the parameter update subsystem, high-order neural observer subsystem, and output-feedback consensus maneuvering control subsystem. For the uncertain MIMO multiagent systems, the proposed control method guarantees distributed consensus maneuvering and input-to-state stability without the need for complete state information. In comparison with the existing literature on leader-following consensus control, maneuvering control, and output-feedback cooperaitve control, the contributions and novelties of the proposed method are listed as follows.

1) In contrast to the existing leader-following consensus tracking controllers proposed in [7], [8], [9], [10], [11], [12], [13], [14], [15], [16], and [17] guided by time-dependent trajectories, the proposed distributed neural observer-based adaptive control method is developed for output-feedback consensus maneuvering along the parameterized path herein. Specifically, output-feedback consensus maneuvering can be regarded as a general case of output-feedback consensus tracking.
2) In contrast to the maneuvering control methods in [18], [19], [20], [21], [22], [23], [24], [25], [26], [27], [28], [29], and [30] that rely on full-state information, the proposed distributed neural observer-based adaptive control method is formulated using only the output information. Furthermore, compared with the existing maneuvering control methods in [18], [19], [20], [21], [22], [23], [24], [25], [26], [27], [28], [29], and [30], which primarily focus on the second-order dynamic task, the dynamic task considered in this article is of the nth-order, representing a more general case for maneuvering control.
3) In contrast to the observer-based adaptive control methods developed in [35], [36], [37], [38], and [39] for output-feedback coordination of the nth-order dynamics, which employ adaptive backstepping or dynamic surface control design involving n approximators and control laws, the proposed distributed neural observer-based adaptive control method for consensus maneuvering simplifies complexity by reformulating the model and reducing the number of approximators and control laws to just one. The proposed method maintains the dimension of approximators and control laws.

The remainder of this article is organized as follows. Section II introduces some preliminary knowledge and problem statements briefly. Section III elaborates on the proposed distributed neural observer-based adaptive control method. Section IV analyzes the stability. In Section V, the effectiveness of the proposed distributed neural observer-based adaptive control method for output consensus maneuvering is demonstrated through simulation.

II. Preliminaries and Problem Statement

This section briefly introduces the notations and graph theory, derives the dynamics of uncertain MIMO strict-feedback multiagent systems, and describes the output-feedback consensus maneuvering problem.

A. Notations

In this article, let $\underline{\sigma}(\cdot)$ and $\bar{\sigma}(\cdot)$ be the minimal and maximal eigenvalues of a matrix, respectively. Let $\bar{\lambda}(\cdot)$ be the maximal singular value of a matrix. Let rank$(\cdot)$ denote the rank of a matrix. Let diag$\{\cdot\}$ be a diagonal matrix. An m by m unitary matrix is represented as I_m. O_m denotes an m by m zero matrix. An m-dimensional column vector consisting of 1 is represented as $\mathbf{1}_m$. An m-dimensional column vector consisting of 0 is represented as $\mathbf{0}_m$. row$_i(\cdot)$ denotes the ith row of a matrix. sgn$(\cdot) = [\text{sign}(\cdot), \ldots, \text{sign}(\cdot)]^T$ with sign$(\cdot)$ being a sign function. $\mathbb{R}^n$ denotes the n-dimensional Euclidean Space. $\mathbb{R}^+$ denotes the positive real scalar. $f^{(l)}(\cdot)$ denotes the lth-order derivative of $f(\cdot)$. $\|\cdot\|$ and $\|\cdot\|_{\mathrm{F}}$ denote the Euclidean norm and the Frobenius norm, respectively. $\otimes$ represents the Kronecker product.

B. Graph Theory

Define $\mathcal{G} = (\mathcal{V}, \mathcal{W})$ as a directed graph for M agents. $\mathcal{V} = (n_1, \ldots, n_M)$ and $\mathcal{W} = \{(n_i, n_j) \in \mathcal{V} \times \mathcal{V}\}$ represent a vertex set and an edge set, respectively, where n_i denotes the ith node. Let an adjacency matrix associated with $\mathcal{G}$ be $\mathcal{A} = [a_{i,j}] \in \mathbb{R}^{M\times M}$ for followers. $a_{i,j} = 1$ means $(n_j, n_i) \in \mathcal{W}$, and $a_{i,j} = 0$ denotes $(n_j, n_i) \notin \mathcal{W}$ or $i = j$. Define $D = \text{diag}\{d_1, \ldots, d_M\}$ as a degree matrix associated with $\mathcal{G}$, where $d_i = \sum a_{i,j}$. Define $\mathcal{L} = D - \mathcal{A}$ as a Laplacian matrix associated with $\mathcal{G}$. Define a spanning matrix $\mathcal{B} = \text{diag}\{b_1, \ldots, b_M\}$ for the virtual leader where $b_i = 1$ denotes that the ith follower communicates with the virtual leader; otherwise, $b_i = 0$. Define two auxiliary matrices $\mathcal{H} = \mathcal{B} + \mathcal{L}$, and $\mathcal{H}'$, where row$_i(\mathcal{H}') =$ row$_i(\mathcal{H})$ when $b_i = 1$ otherwise row$_i(\mathcal{H}') = \mathbf{0}_M^T$.

Assumption 1 [40]: There is a spanning tree in $\mathcal{G}$ with the root node serving as the leader. This implies the existence of a directed path from the leader to each follower.

Lemma 1 [40]: Under Assumption 1, the matrix $\mathcal{H}$ is nonsingular. Moreover, all eigenvalues of $\mathcal{H}$ are in the open right-half plane.

Lemma 2 [41]: Under Assumption 1, define

$$\begin{aligned} q &= [q_1, \ldots, q_M]^T = \mathcal{H}^{-1}\mathbf{1}_M \\ \mathcal{T} &= \text{diag}\{\tau_1, \ldots, \tau_M\} = \text{diag}\left\{\frac{1}{q_1}, \ldots, \frac{1}{q_1}\right\} \\ G &= \mathcal{H}^T\mathcal{T} + \mathcal{T}\mathcal{H} \end{aligned} \tag{1}$$

where G and $\mathcal{T}$ are positive definite.

C. System and Problem Statement

The uncertain MIMO strict-feedback multiagent system considered in this article consists of M followers. The model of the ith follower is

$$\begin{cases} \dot{x}_{i,k} = x_{i,k+1} + f_{i,k}(\bar{x}_{i,k}) \\ \dot{x}_{i,n} = u_i + f_{i,n}(\bar{x}_{i,n}) + w_i(t) \\ y_i = x_{i,1} \end{cases} \tag{2}$$

where $i = 1, 2, \ldots, M$, $k = 1, \ldots, n-1$, $x_{i,l} \in \mathbb{R}^m$ represents the state, $l = 1, \ldots, n$, $\bar{x}_{i,l} = [x_{i,1}^T, \ldots, x_{i,l}^T]^T \in \mathbb{R}^{lm}$, $u_i \in \mathbb{R}^m$ is the input, $y_i \in \mathbb{R}^m$ is the output, $f_{i,l}(\bar{x}_i) \in \mathbb{R}^m$ denotes a smooth and bounded uncertain nonlinear term, and $w_i(t) \in \mathbb{R}^m$ denotes external disturbances.

According to [42], the system model (2) can be reformulated by using $y_i^{(n)}$, allowing to transform (2) into the following form:

$$\begin{cases} \dot{x}_{i,1} = s_{i,2} \\ \dot{s}_{i,k} = s_{i,k+1} \\ \dot{s}_{i,n} = u_i + g_i(\bar{x}_{i,n}, t) \end{cases} \tag{3}$$

where $k = 2, \ldots, n-1$, $s_{i,2} = x_{i,2} + f_{i,1}(x_{i,1})$, $s_{i,k+1} = x_{i,k+1} + \sum_{l=1}^{k-1}([d^{k-l}f_{i,l}(\bar{x}_{i,l})]/[dt^{k-l}]) + f_{i,k}(\bar{x}_{i,k})$, and $g_i(\bar{x}_{i,n}, t) = \sum_{l=1}^{n-1}([d^{n-l}f_{i,l}(\bar{x}_{i,l})]/[dt^{n-l}]) + f_{i,n}(\bar{x}_{i,n}) + w_i(t)$.

Furthermore, letting $S_i = [x_{i,1}^T, s_{i,2}^T, \ldots, s_{i,n}^T]^T$, the dynamics of the ith follower governed by (3) can be transformed into the following form:

$$\begin{cases} \dot{S}_i = AS_i + B(u_i + g_i(\bar{x}_{i,n}, t)) \\ y_i = CS_i \end{cases} \tag{4}$$

where

$$A = \begin{bmatrix} O_m & I_m & O_m & \cdots & O_m \\ O_m & O_m & I_m & \cdots & O_m \\ \vdots & \vdots & \ddots & \vdots & \vdots \\ O_m & O_m & O_m & \cdots & O_m \end{bmatrix} \in \mathbb{R}^{mn\times mn}$$

$$B = \begin{pmatrix} O_m \\ \vdots \\ O_m \\ I_m \end{pmatrix} \in \mathbb{R}^{mn\times m}$$

$$C = \begin{bmatrix} I_m & O_m & O_m & \cdots & O_m \end{bmatrix} \in \mathbb{R}^{m\times mn}.$$

Remark 1: For the system (2), the following neural observer is always constructed to design the output-feedback controller:

$$\begin{cases} \dot{\hat{x}}_{i,k} = \hat{x}_{i,k+1} + \hat{W}_{i,k}^T X_{i,k} - \kappa_{i,1}(\hat{y}_i - y_i) \\ \dot{\hat{x}}_{i,n} = u_i + \hat{W}_{i,n}^T X_{i,n} - \kappa_{i,n}(\hat{y}_i - y_i) \\ \hat{y}_i = \hat{x}_{i,1}. \end{cases} \tag{5}$$

On the one hand, when designing output-feedback neural adaptive controllers, the construction of n neural networks and adaptation laws is necessary. As the system order increases, these neural networks contribute to a higher computational burden. On the other hand, regulating the neural observer (5) becomes challenging due to the nonlinearity present in each order dynamics of (5), encompassing the approximator $\hat{W}_{i,l}^T X_{i,l}$ and the next-order estimated state $\hat{x}_{i,l}$. These challenges render output-feedback control more demanding than state-feedback control. However, upon transforming the system model (2) into (3), the number of neural networks and adaptation laws can be reduced to just one, and the dynamics of the proposed observer (22) from the first-order to the $(n-1)$th-order

become linear. Therefore, model transformation simplifies the design complexity of output-feedback controllers. Moreover, nonbackstepping control methods can be applied to uncertain nonlinear systems after the model transformation [42], [43].

In the consensus maneuvering problem considered herein, the parameterized path $y_r(\theta)$ is preloaded into one of the followers, designating it as the leader within the swarm. The virtual leader follows a parameterized path $y_r(\theta) \in \mathbb{R}^m$, where $\theta \in \mathbb{R}$ denotes a path variable. The information related to the virtual leader is accessible only to a select few followers.

Let $Y_r = [y_r^T(\theta), (dy_r^T(\theta)/dt), \ldots, (d^{n-1}y_r^T(\theta)/dt^{n-1})]^T$, the dynamics of Y_r is represented as

$$\dot{Y}_r = AY_r + B\left[f_r(\theta, y_r(\theta)) + y_r^{\theta}(\theta)\omega\right] \tag{6}$$

where $f_r(\theta, y_r(\theta)) \in \mathbb{R}^m$ denotes a bounded function with respect to the $l(l = 1, \ldots, n-2)$th-order derivative of θ and $y_r(\theta)$, $y_r^{\theta}(\theta) \in \mathbb{R}^m$ denotes the first-order partial derivative along θ and ω is a to-be-designed parameter. For the virtual leader, an assumption is made as follows.

Assumption 2: The path $y_r(\theta)$ and its lth-order partial derivative $y_r^{(l)}(\theta)$ are bounded, where $l = 1, \ldots, n$. $f_r(\theta, y_r(\theta))$ is bounded with $f_{rM} \in \mathbb{R}^+$ satisfying $\|f_r(\cdot)\| \le f_{rM}$.

Problem: For the multiagent system (2) and the virtual leader (6), the control objective is to derive a distributed output-feedback consensus maneuvering controller utilizing output information y_i as well as virtual leader information Y_r and θ_{ref}. This distributed output-feedback consensus maneuvering controller comprises an approximation term $\hat{f}_i$, a control law u_i, a high-order neural observer $\dot{\hat{S}}_i$, an adaptation law $\dot{\hat{W}}_i$, and an update law $\dot{\omega}$, given by

$$\begin{aligned}
\hat{f}_i &= \hat{W}_i^T X_i \\
u_i &= \psi_{u,i}\left(\hat{S}_i, Y_r, \hat{S}_j, \hat{f}_i\right),\ j \in \mathcal{F}_i \\
\dot{\hat{S}}_i &= \psi_{\hat{S},i}\left(\hat{S}_i, y_i, u_i, \hat{f}_i\right) \\
\dot{\hat{W}}_i &= \psi_{\hat{W},i}\left(\hat{S}_i, y_i, \hat{W}_i\right) \\
\dot{\omega} &= \psi_{\omega,i}\left(\hat{S}_i, Y_r, \theta, \theta_{\text{ref}}\right)
\end{aligned}$$

such that the following geometric and dynamic tasks are satisfied.

Geometric Task [18], [44]: All followers are driven to agree on a common motion governed by the parameterized path $y_r(\theta)$ as

$$\lim_{t\to\infty} \|y_i - y_r(\theta)\| \le \delta_g$$

where there exists $\delta_g \in \mathbb{R}^+$ as a small residual error.

Dynamic Task [18], [44]: Define $\theta_a = [\theta, \dot{\theta}, \ldots, \theta^{(n-1)}]^T$. For the virtual leader, the update speed of the path variable is non-negative such that $\dot{\theta} \ge 0$. Moreover, θ_a is driven to converge to a given dynamic specification $\theta_{\text{ra}} = [\theta_{\text{ref}}(t), \dot{\theta}_{\text{ref}}(t), \ldots, \theta_{\text{ref}}^{(n-1)}(t)]^T \in \mathbb{R}^n$ as follows:

$$\lim_{t\to\infty} \|\theta_a - \theta_{\text{ra}}\| \le \delta_d$$

where there exists $\delta_d \in \mathbb{R}^+$ as a small residual error.

Finally, the input-to-state stability small-gain theorem is introduced as follows.

Lemma 3 [45]: Consider the following two subsystems:

$$\begin{aligned}
\dot{x}_1 &= f_1(t, x_1, x_2, u_1) \\
\dot{x}_2 &= f_2(t, x_2, x_1, u_2).
\end{aligned}$$

The subsystem x_1 and the subsystem x_2 are input-to-state stable with (x_2, u_1) and (x_1, u_2) as inputs, respectively. There exist $\mathcal{KL}$ functions $\beta_{x_1}(\cdot)$ and $\beta_{x_2}(\cdot)$ and $\mathcal{K}_\infty$ functions $\kappa_{x_2}(\cdot)$, $\kappa_{u_1}(\cdot)$, $\kappa_{x_1}(\cdot)$, and $\kappa_{u_2}(\cdot)$ satisfying

$$\begin{aligned}
\|x_1(t)\| &\le \beta_{x_1}(\|x_1(0)\|, t) + \kappa_{x_2}(\|x_2\|) + \kappa_{u_1}(\|u_1\|) \\
\|x_2(t)\| &\le \beta_{x_2}(\|x_2(0)\|, t) + \kappa_{x_1}(\|x_1\|) + \kappa_{u_2}(\|u_2\|).
\end{aligned}$$

If the condition

$$\kappa_{x_2} \circ \kappa_{x_1}(r) < r \text{ or } \kappa_{x_1} \circ \kappa_{x_2}(r) < r \quad \forall r > 0$$

holds, the interconnection system formed by x_1 and x_2 is input-to-state stable.

III. Distributed Neural Observer-Based Adaptive Control Method for Output-Feedback Consensus Maneuvering

In this section, a distributed observer-based neural adaptive control method is proposed based on the modular design approach to ensure output-feedback consensus maneuvering. This method encompasses a path update law, a high-order neural observer, and an output-feedback consensus maneuvering control law.

A. Path Update Law

In this section, a path update law is developed for the leader to guarantee the dynamic task. First, consider the nth-order dynamics of θ as

$$\theta^{(n)} = \omega \tag{7}$$

where $\omega \in \mathbb{R}$ is a to-be-designed variable.

Letting $\theta_a = [\theta, \dot{\theta}, \ddot{\theta}, \ldots, \theta^{(n-1)}]^T$, (7) is expressed by the state model

$$\dot{\theta}_a = A_p\theta_a + B_p\omega \tag{8}$$

where

$$B_p = \begin{pmatrix} 0 \\ \vdots \\ 0 \\ 1 \end{pmatrix} \in \mathbb{R}^n, \quad A_p = \begin{bmatrix} 0 & 1 & 0 & \cdots & 0 \\ 0 & 0 & 1 & \cdots & 0 \\ \vdots & \vdots & \ddots & \vdots & \vdots \\ 0 & 0 & 0 & \cdots & 0 \end{bmatrix} \in \mathbb{R}^{n\times n}.$$

Then, ω is produced by the following form:

$$\dot{\omega} = -\lambda_l\omega + \hat{\omega} \tag{9}$$

where $\lambda_l \in \mathbb{R}^+$ denotes a tuning parameter, and $\hat{\omega} \in \mathbb{R}$ is a to-be-designed variable.

Merging (9) into (8) and letting $\bar{\theta}_a = [\theta, \dot{\theta}, \ddot{\theta}, \ldots, \theta^{(n-1)}, \omega]^T$, the new state model is expressed by the following form:

$$\dot{\bar{\theta}}_a = A_l\bar{\theta}_a + B_l\hat{\omega} \tag{10}$$

where

$$B_l = \begin{pmatrix} 0 \\ \vdots \\ 0 \\ 1 \end{pmatrix} \in \mathbb{R}^{n+1}$$

and

$$A_l = \begin{bmatrix} 0 & 1 & 0 & \cdots & 0 \\ 0 & 0 & 1 & \cdots & 0 \\ \vdots & \vdots & \ddots & \vdots & \vdots \\ 0 & 0 & 0 & \cdots & 1 \\ 0 & 0 & 0 & \cdots & -\lambda_l \end{bmatrix} \in \mathbb{R}^{(n+1)\times(n+1)}.$$

An update law of ω is constructed as follows:

$$\begin{cases} \dot{\omega} = -\lambda_l \omega + \hat{\omega} \\ \hat{\omega} = -c_l B_l^T P_l \big(\bar{\theta} - \bar{\theta}_{\mathrm{ra}}\big) + h_\omega \\ h_\omega = -\sum_{i\in\mathcal{N}_l} b_i \rho_l y_r^{\theta T}(\theta)\big(C\hat{e}_i\big) \end{cases} \tag{11}$$

where $\bar{\theta}_{\mathrm{ra}} = [\theta_{\mathrm{ra}}^T, 0]^T$, $\theta_{\mathrm{ra}} = [\theta_{\mathrm{ref}}(t), \dot{\theta}_{\mathrm{ref}}(t), \ldots, \theta_{\mathrm{ref}}^{(n-1)}(t)]^T \in \mathbb{R}^n$ is the given dynamic specification, $c_l \in \mathbb{R}^+$ is a coupling gain, $\rho_l \in \mathbb{R}^+$ denotes a tuning parameter, $\mathcal{N}_l$ is the neighbor set of the leader, $P_l = P_l^T \in \mathbb{R}^{(n+1)\times(n+1)}$ is a positive-definite solution through solving the following algebraic Riccati inequality with $Q_l = Q_l^T \in \mathbb{R}^{(n+1)\times(n+1)}$ being a positive-definite matrix:

$$P_l A_l + A_l^T P_l - P_l B_l B_l^T P_l + Q_l < 0 \tag{12}$$

and an estimated consensus maneuvering error $\hat{e}_i$ is defined as follows:

$$\hat{e}_i = \sum_{j\in\mathcal{F}_i} a_{i,j}\Big(\hat{S}_i - \hat{S}_j\Big) + b_i\Big(\hat{S}_i - Y_r\Big)$$

where $\mathcal{F}_i$ denotes the neighbor set of the ith follower.

The solvable problem of (12) can be determined by analyzing the controllability of the pair (A_l, B_l). Because the controllability matrix $M_l = (B_l, A_l B_l, A_l^2 B_l, \ldots, A_l^n B_l)$ is equal to

$$M_l = \begin{bmatrix} 0 & 0 & 0 & \cdots & 1 \\ 0 & 0 & 0 & \cdots & (-\lambda_l) \\ \vdots & \vdots & \ddots & \vdots & \vdots \\ 0 & 1 & (-\lambda_l) & \cdot & (-\lambda_l)^{n-2} \\ 1 & (-\lambda_l) & (-\lambda_l)^2 & \cdots & (-\lambda_l)^{n-1} \end{bmatrix} \in \mathbb{R}^{(n+1)\times(n+1)}$$

it can be observed that $\mathrm{rank}(M_l) = n+1$. Therefore, (12) is solvable.

Define $\tilde{\theta}_a = \theta_a - \theta_{\mathrm{ra}}$ and $\tilde{\bar{\theta}}_a = \bar{\theta}_a - \bar{\theta}_{\mathrm{ra}} = [\tilde{\theta}_a^T, \omega]^T$. The subsystem Σ_l governed by $\tilde{\theta}_a$ and ω is given as follows:

$$\Sigma_l: \begin{cases} \dot{\tilde{\bar{\theta}}}_a = A_l \tilde{\bar{\theta}}_a + B_l \hat{\omega} \\ \hat{\omega} = -c_l B_l^T P_l \tilde{\bar{\theta}}_a + h_\omega \\ h_\omega = -\sum_{i\in\mathcal{N}_l} b_i \rho_l y_r^{\theta T}(\theta)\big(C\hat{e}_i\big). \end{cases} \tag{13}$$

An estimated local tracking error for the ith follower can be defined as $\hat{\delta}_i = \hat{S}_i - Y_r$. The next lemma demonstrates the stability property of the subsystem Σ_l.

Lemma 4: Consider the subsystem Σ_l governed by (13) with states being $\tilde{\theta}_a$ and ω and the input being $\hat{\delta}$. If Assumptions 1 and 2 hold and $c_l \geq 1/2$, Σ_l is input-to-state stable

Proof: Taking

$$V_l = \frac{1}{2}\tilde{\bar{\theta}}_a^T P_l \tilde{\bar{\theta}}_a \tag{14}$$

as a positive-definite Lyapunov function candidate, we obtain

$$\begin{aligned} \dot{V}_l = {} & \frac{1}{2}\tilde{\bar{\theta}}_a^T (A_l^T P_l + P_l A_l - 2c_l P_l B_l^T B_l P_l)\tilde{\bar{\theta}}_a \\ & - \tilde{\bar{\theta}}_a^T B_l \sum_{i\in\mathcal{N}_l} b_i \rho_l y_r^{\theta T}(\theta)(C\hat{e}_i). \end{aligned} \tag{15}$$

Using (12) and defining $\hat{\delta} = [\hat{\delta}_1^T, \ldots, \hat{\delta}_M^T]^T \in \mathbb{R}^{Mmn}$, (15) can be further put into

$$\begin{aligned} \dot{V}_l = {} & \frac{1}{2}\tilde{\bar{\theta}}_a^T \big(A_l^T P_l + P_l A_l - 2c_l P_l B_l^T B_l P_l\big)\tilde{\bar{\theta}}_a \\ & - \rho_l \tilde{\bar{\theta}}_a^T B_l y_r^{\theta T}(\theta)\big((\mathcal{H}'\mathbf{1}_M)^T \otimes C\big)\hat{\delta} \\ \leq {} & -\frac{\underline{\sigma}(Q_l)}{2}\|\tilde{\bar{\theta}}_a\|^2 + \rho_l \bar{y}_r^{\theta}\bar{\sigma}\big(\mathcal{H}'\big)\|\tilde{\bar{\theta}}_a\|\|\hat{\delta}\|. \end{aligned} \tag{16}$$

Letting $E_l = [\|\tilde{\theta}_a\|, |\omega|]^T$, (16) is transformed into the following form:

$$\dot{V}_l \leq -c_1\|E_l\|^2 + \rho_l c_2 \|E_l\|\|\hat{\delta}\| \tag{17}$$

where $c_1 = 0.5\underline{\sigma}(Q_l)$ and $c_2 = \bar{y}_r^{\theta}\bar{\sigma}(\mathcal{H}')$.

Since $\|E_l\| \geq 2\rho_l c_2\|\hat{\delta}\|/c_1$ makes

$$\dot{V}_c \leq -\frac{1}{2}c_1\|E_l\|^2 \tag{18}$$

the subsystem Σ_l governed by (13) is input-to-state stable. Letting $\Psi_l = \mathrm{diag}\{P_l, 1\}$, there exist a class $\mathcal{KL}$ function $\beta_l(\cdot)$ and a class $\mathcal{K}$ function $\kappa_{\hat{\delta}}(\cdot)$. Consequently

$$\|E_l(t)\| \leq \beta_l(\|E_l(0)\|, t) \quad + \kappa_{\hat{\delta}}\Big(\|\hat{\delta}\|\Big) \tag{19}$$

where $\kappa_{\hat{\delta}}(r) = 2\rho_l c_2\sqrt{\bar{\sigma}(\Psi_l)}r/c_1\sqrt{\underline{\sigma}(\Psi_l)}$. ■

B. High-Order Neural Observer

In this section, a high-order neural observer is designed for the ith follower to estimate unknown states, by integrating an echo state network as the approximator. First, let us recall the dynamics of S_i as follows:

$$\dot{S}_i = AS_i + B\big[u_i + g_i\big(\bar{x}_{i,n}, t\big)\big]. \tag{20}$$

To estimate the uncertain term $g_i(\bar{x}_{i,n}, t)$, the following echo state network is taken [46]:

$$g_i\big(\bar{x}_{i,n}, t\big) = W_i^T X_i + \varepsilon_i(t) \tag{21}$$

where $W_i \in \mathbb{R}^{p\times m}$ denotes a weight matrix satisfying $\|W_i\|_{\mathrm{F}} \leq W_i^*$ with $W_i^* \in \mathbb{R}^+$, $\varepsilon_i(t) \in \mathbb{R}^m$ is an approximation error satisfying $\|\varepsilon_i(t)\| \leq \varepsilon_i^*$ with $\varepsilon_i^* \in \mathbb{R}^+$, and $X_i \in \mathbb{R}^p$ is a p-dimensional reservoir state, and $\dot{X}_i$ is given by

$$\dot{X}_i = c_i\big[-h_i X_i + \phi_i\big(W_{i,\xi_i}\xi_i + W_{i,X_i}X_i\big)\big]$$

where $\xi_i = [y_i^T(t), y_i^T(t-t_d), \ldots, y_i^T(t-nt_d), u_i^T(t)]^T \in \mathbb{R}^{(n+2)m}$, $c_i \in \mathbb{R}^{p\times p}$ is a time constant matrix, $h_i \in \mathbb{R}^{p\times p}$ is a tuning parameter matrix, $\phi_i(\cdot) \in \mathbb{R}^p$ represents an activation function, and $W_{i,\xi_i} \in \mathbb{R}^{p\times(n+2)m}$ and $W_{i,X_i} \in \mathbb{R}^{p\times p}$ are internal

weight matrices. Note that alternative approximators, such as various types of neural networks and fuzzy-logic systems, can also be employed.

Then, a high-order neural observer for S_i is developed as

$$\begin{cases} \dot{\hat{S}}_i = A\hat{S}_i + B\left(u_i + \hat{W}_i^T X_i\right) - F\left(\hat{y}_i - y_i\right) \\ \dot{\hat{W}}_i = -\Gamma_i\left(X_i(\hat{y}_i^T - y_i^T) + k_{W_i}\hat{W}_i\right) \\ \hat{y}_i = C\hat{S}_i \end{cases} \tag{22}$$

where $\hat{S}_i \in \mathbb{R}^{mn}$ is an estimated state of S_i, $F \in \mathbb{R}^{mn\times m}$ denotes an observer gain matrix, $\Gamma_i \in \mathbb{R}^{m\times m}$ denotes an positive adaptation gain, and $k_{W_i} \in \mathbb{R}^{m\times m}$ is a tuning parameter.

Letting $\tilde{S}_i = \hat{S}_i - S_i$ and $\tilde{W}_i = \hat{W}_i - W_i$, the dynamics of $\tilde{S}_i$ and $\tilde{W}_i$ is represented as

$$\Sigma_{o,i}: \begin{cases} \dot{\tilde{S}}_i = A_{o,i}\tilde{S}_i + B\left(\tilde{W}_i^T X_i - \varepsilon_i(t)\right) \\ \dot{\tilde{W}}_i = -\Gamma_i\left[X_i\left(\tilde{S}_i^T C^T\right) + K_{W_i}\hat{W}_i\right] \end{cases} \tag{23}$$

where $A_o = A - FC$. There exists the following algebraic Riccati inequality:

$$\begin{aligned} &A_o^T P_{o,i} + P_{o,i}A_o + Q_{o,i} \\ &\quad + P_{o,i}BB^T P_{o,i} + \iota_i R_{o,i}R_{o,i}^T < 0 \end{aligned} \tag{24}$$

where $\iota_i \in \mathbb{R}^+$ is a tuning parameter, $Q_{o,i} = Q_{o,i}^T \in \mathbb{R}^{mn\times mn}$ denotes a positive-definite matrix, and $R_{o,i} = P_{o,i}B - C^T$ with $P_{o,i} = P_{o,i}^T \in \mathbb{R}^{mn\times mn}$ being a positive-definite solution through solving the algebraic Riccati inequality (24).

The solvable problem of (24) can be transformed into the solvability of the following matrix inequality:

$$\begin{bmatrix} A_o^T P_{o,i} + P_{o,i}A_o + Q_{o,i} + \iota_i R_{o,i}R_{o,i}^T & P_{o,i}B \\ B^T P_{o,i} & -I_m \end{bmatrix} < 0 \tag{25}$$

and it can be solved based on the *Schur Complement Lemma* [47]. When A_o is Hurwtiz, $A_o^T P_{o,i} + P_{o,i}A_o + Q_{o,i} + \iota_i R_{o,i}R_{o,i}^T$ is similar to the Lyapunov matrix inequality such that (25) is solvable. To reduce the dimension of matrices, define $A_o = A - FC = (A_p - F_pC_p) \otimes I_m = \bar{A}_o \otimes I_m$ and $B = B_p \otimes I_m$ with $\bar{A}_o = A_p - F_pC_p$, $F = F_p \otimes I_m$, and $C = C_p \otimes I_m$. An n-dimensional matrix $\bar{A}_o$ can be used as the judging condition rather than the mn-dimensional matrix A_o. The form of $\bar{A}_o$ is

$$\bar{A}_o = \begin{bmatrix} -r_1 & 1 & 0 & \cdots & 0 \\ -r_2 & 0 & 1 & \cdots & 0 \\ \vdots & \vdots & \ddots & \vdots & \vdots \\ -r_n & 0 & 0 & \cdots & 0 \end{bmatrix} \in \mathbb{R}^{n\times n}.$$

We can choose the appropriate parameters for $F_p = [r_1, \ldots, r_n]^T \in \mathbb{R}^n$ to make $\bar{A}_o$ being Hurwtiz. Under this condition, (24) is solvable.

Next, the following lemma demonstrates the stability property of the subsystem $\Sigma_{o,i}$.

Lemma 5: Consider the subsystem $\Sigma_{o,i}$ governed by (23) with inputs being ε_i and W_i and states being $\tilde{S}_i$ and $\tilde{W}_i$. If Assumptions 1 and 2 hold and $\underline{\sigma}(K_{W_i}) - X_i^{*2}/\iota_i > 0$, $\Sigma_{o,i}$ is input-to-state stable.

Proof: Consider the following positive-definite Lyapunov function candidate:

$$V_{o,i} = \tilde{S}_i^T P_{o,i}\tilde{S}_i + \mathrm{tr}\left(\tilde{W}_i^T \Gamma_i^{-1}\tilde{W}_i\right). \tag{26}$$

The time derivative of $V_{o,i}$ along (23) satisfies

$$\begin{aligned} \dot{V}_{o,i} = {} & \tilde{S}_i^T(A_o^T P_{o,i} + P_{o,i}A_o)\tilde{S}_i + 2\tilde{S}_i^T R_{o,i}(\tilde{W}_i^T X_i) \\ & + 2\tilde{S}_i^T P_{o,i}B\varepsilon_i - 2[\mathrm{tr}(\tilde{W}_i^T K_{W_i}\tilde{W}_i) \\ & + \mathrm{tr}(\tilde{W}_i^T K_{W_i}W_i)]. \end{aligned} \tag{27}$$

By using the following Young's inequalities:

$$\begin{cases} \tilde{S}_i^T R_{o,i}\left(\tilde{W}_i^T X_i\right) \le \frac{\iota_i \tilde{S}_i^T R_{o,i}R_{o,i}^T\tilde{S}_i}{2} + \frac{\tilde{W}_i^T X_i X_i^T\tilde{W}_i}{2\iota_i} \\ -\tilde{S}_i^T P_{o,i}B\varepsilon_i \le \frac{\tilde{S}_i^T P_{o,i}BB^T P_{o,i}\tilde{S}_i}{2} + \frac{\varepsilon_i^T\varepsilon_i}{2} \\ \mathrm{tr}\left(\tilde{W}_i^T K_{W_i}W_i\right) \le \frac{\mathrm{tr}\left(\tilde{W}_i^T K_{W_i}\tilde{W}_i\right)}{2} + \frac{\mathrm{tr}\left(W_i^T K_{W_i}W_i\right)}{2}. \end{cases} \tag{28}$$

$\dot{V}_{o,i}$ can be further put into

$$\begin{aligned} \dot{V}_{o,i} \le {} & -\underline{\sigma}\left(Q_{o,i}\right)\|\tilde{S}_i\|^2 - \left(\underline{\sigma}(K_{W_i}) - \frac{X_i^{*2}}{\iota_i}\right)\|\tilde{W}_i\|_{\mathrm{F}}^2 \\ & + \|\varepsilon_i\|^2 + \bar{\sigma}\left(K_{W_i}\right)\|W_i\|_{\mathrm{F}}^2 \\ \le {} & -c_{i,3}\|E_{o,i}\|^2 + \|U_{o,i}\|^2 \end{aligned} \tag{29}$$

where $E_{o,i} = [\|\tilde{S}_i\|, \|\tilde{W}_i\|_{\mathrm{F}}]^T$, $U_{o,i} = [\|\varepsilon_i\|, \sqrt{\bar{\sigma}(K_{W_i})}\|W_i\|_{\mathrm{F}}]^T$, and $c_{i,3} = \min\{\underline{\sigma}(Q_{o,i}), \underline{\sigma}(K_{W_i}) - X_i^{*2}/\iota_i\}$.

Since $\|E_{o,i}\| \ge 2\|U_{o,i}\|/c_{i,3}$ makes

$$\dot{V}_{o,i} \le -\frac{c_{i,3}}{2}\|E_{o,i}\|^2 \tag{30}$$

the subsystem $\Sigma_{o,i}$ can be proved to be input-to-state stable. There exists a class $\mathcal{KL}$ function $\beta_{o,i}(\cdot)$ and two class $\mathcal{K}$ functions $\kappa_{\varepsilon_i}(\cdot)$ and $\kappa_{W_i}(\cdot)$. Consequently

$$\begin{aligned} \|E_{o,i}(t)\| \le {} & \beta_{o,i}\left(\|E_{o,i}(0)\|, t\right) + \kappa_{\varepsilon_i}(\|\varepsilon_i\|) \\ & + \kappa_{W_i}(\|W_i\|_{\mathrm{F}}) \end{aligned} \tag{31}$$

where $\kappa_{\varepsilon_i}(r) = 2\sqrt{\bar{\sigma}(\Phi_{o,i})}r/c_{i,3}\sqrt{\underline{\sigma}(\Phi_{o,i})}$ and $\kappa_{W_i}(r) = 2\sqrt{\bar{\sigma}(\Phi_{o,i})\bar{\sigma}(K_{W_i})}r/c_{i,3}\sqrt{\underline{\sigma}(\Phi_{o,i})}$ with $\Phi_{o,i} = \mathrm{diag}\{1, \Gamma_i^{-1}\}$. ■

Remark 2: According to *Weierstrass Approximation Theorem*, suppose $g_i(\cdot)$ to be a continuous real-valued function defined on the real interval. $g_i(\cdot)$ can be uniformly approximated by a sequence of polynomials. This implies that $g_i(\cdot)$ should be a continuous and continuously differentiable function defined in a compact set, such that $g_i(\cdot)$ is smooth. If the agent is not subject to some additional constraints, such as faults and malicious attacks, the boundedness of states $\bar{x}_{i,n}$ is easily ensured under the degenerative feedback in the steady-state stage, such that $g_i(\cdot)$ can maintain smooth. It is important to note that some methods have been proposed to investigate neural adaptive control for uncertain nonlinear systems subject to nonsmooth dynamics. Zhao et al. [48] decomposed the nonsmooth uncertain dynamics subject to finite jumps into a continuous term and a noncontinuous approximation error based on the *Cellina Approximate Selection Theorem*. Thus, the continuous term can be approximated using neural networks.

Remark 3: The approximation form of the neural network is $g_i(\bar{x}_{i,n}, t) = W_i^T X_i + \varepsilon_i(t)$, where $\varepsilon_i(t)$ represents an approximation error. $g_i(\bar{x}_{i,n}, t)$ can be regarded as a nonlinear function that encompasses both parametric and nonparametric uncertainties, as discussed in [49]. This is different from the full feedback linearizable adaptation considered in [50] and [51], where unlinearizable (or nonparametric) uncertainties can be integrated into the approximation error. The lower the continuity, the poorer the learning profile.

Remark 4: To ensure that states remain within the compact set, the following approaches can be employed. First, appropriate initial values for the states need to be set. Second, a higher control gain can be utilized to shorten the transient process. Third, a smaller adaptation gain can be employed to reduce the overshoot of estimated weights. In practice, these approaches are often used in combination.

C. Consensus Maneuvering Control Law

A consensus maneuvering control law is constructed for the ith follower to stabilize the closed-loop system. First, recall the estimated consensus maneuvering error $\hat{e}_i$ as follows:

$$\hat{e}_i = \sum_{j\in\mathcal{F}_i} a_{i,j}\left(\hat{S}_i - \hat{S}_j\right) + b_i\left(\hat{S}_i - Y_r\right).$$

To stabilize the dynamics of S_i, a control law u_i can be designed for the ith follower as

$$u_i = -c_u K\hat{e}_i - \hat{W}_i^T X_i - f_{rM}\mathrm{sgn}\left(K\hat{e}_i\right) \tag{32}$$

where $c_u \in \mathbb{R}^+$ is a coupling gain, and $K \in \mathbb{R}^{m\times mn}$ denotes a feedback gain matrix and is taken as

$$K = B^T P_c$$

where $P_c = P_c^T \in \mathbb{R}^{mn\times mn}$ is a positive-definite solution satisfying an algebraic Riccati inequality

$$P_c A + A^T P_c + Q_c - P_c BB^T P_c < 0 \tag{33}$$

with $Q_c = Q_c^T \in \mathbb{R}^{mn\times mn}$ being a positive-definite matrix.

Define $A = A_p \otimes I_m$ and $B = B_p \otimes I_m$. The solvable problem of (33) can be determined by analyzing the controllability of the pair (A_p, B_p). Because the controllability matrix $M_p = (B_p, A_pB_p, A_p^2B_p, \ldots, A_p^{n-1}B_p)$ is equal to

$$M_p = \begin{bmatrix} 0 & 0 & 0 & \cdots & 1 \\ 0 & 0 & 0 & \cdots & 0 \\ \vdots & \vdots & \ddots & \vdots & \vdots \\ 0 & 1 & 0 & \cdot & 0 \\ 1 & 0 & 0 & \cdots & 0 \end{bmatrix} \in \mathbb{R}^{n\times n}$$

where $\mathrm{rank}(M_p) = n$. Therefore, (33) is solvable.

Recalling $\hat{\delta}_i = \hat{S}_i - Y_r$, the dynamics of $\hat{\delta}_i$ is expressed as

$$\begin{aligned}\dot{\hat{\delta}}_i = {} & A\delta_i - c_u BK\hat{e}_i - F\left(\hat{y}_i - y_i\right) - f_{rM}\mathrm{sgn}\left(K\hat{e}_i\right) \\ & - B\left[f_r(\theta, y_r(\theta)) + y_r^{\theta}(\theta)\omega\right].\end{aligned} \tag{34}$$

Recalling $\hat{\delta} = [\hat{\delta}_1^T, \ldots, \hat{\delta}_M^T]^T$, $\dot{\hat{\delta}}$ is described as follows:

$$\begin{aligned}\Sigma_c : \dot{\hat{\delta}} = {} & (I_M \otimes A - c_u\mathcal{H}\otimes BK)\hat{\delta} - (I_M \otimes FC)\tilde{S} \\ & - \rho - (\mathbf{1}_M \otimes B)[f_r(\theta, y_r(\theta)) + y_r^{\theta}(\theta)\omega]\end{aligned} \tag{35}$$

where $\rho = [(f_{rM}\mathrm{sgn}(K\hat{e}_1))^T, \ldots, (f_{rM}\mathrm{sgn}(K\hat{e}_M))^T]^T$.

Then, the next lemma demonstrates the stability property of the subsystem Σ_c.

Lemma 6: Consider the subsystem Σ_c governed by (35) with inputs being $\tilde{S}_i$ and ω and the state being $\hat{\delta}$. If Assumptions 1 and 2 hold, Σ_c is input-to-state stable, when the coupling gain c_u satisfies the following condition:

$$c_u \geq \frac{1}{2\min_{i=1,\ldots,M}(\sigma_i(G)q_i)}.$$

Proof: Take a Lyapunov function candidate

$$V_c = \frac{1}{2}\hat{\delta}^T(\mathcal{T}\otimes P_c)\hat{\delta}. \tag{36}$$

We obtain $\dot{V}_c$ as

$$\begin{aligned}\dot{V}_c = {} & \frac{1}{2}\hat{\delta}^T\left[\mathcal{T}\otimes(P_cA + A^TP_c) - 2c_uG\otimes(P_cBB^TP_c)\right]\hat{\delta} \\ & - \hat{\delta}^T(\mathcal{T}\otimes P_cFC)\tilde{S} - \hat{\delta}^T(\mathcal{T}\otimes P_c)\rho \\ & - \hat{\delta}^T(\mathcal{T}\mathbf{1}_M\otimes P_cB)\left[y_r^{\theta}(\theta)\omega + f_r(\theta, y_r(\theta))\right].\end{aligned} \tag{37}$$

Using the following inequality:

$$\begin{cases} -\hat{\delta}^T(\mathcal{T}\otimes P_c)\rho \leq -f_{r,M}\|\hat{\delta}^T(\mathcal{T}\otimes P_c)\|_1 \\ -\hat{\delta}^T(\mathcal{T}\mathbf{1}_M\otimes P_cB)f_r(\theta, y_r(\theta)) \leq f_{r,M}\|\hat{\delta}^T(\mathcal{T}\otimes P_c)\|_1 \end{cases}$$

we have

$$\begin{aligned}\dot{V}_c \leq {} & \frac{1}{2}\hat{\delta}^T[\mathcal{T}\otimes(P_cA + A^TP_c) - 2c_uG\otimes(P_cBB^TP_c)]\hat{\delta} \\ & - c_u\hat{\delta}^T(\mathcal{T}\otimes P_cFC)\tilde{S} \\ & - \delta^T(\mathcal{T}\mathbf{1}_M\otimes P_cB)y_r^{\theta}(\theta)\omega.\end{aligned} \tag{38}$$

Introducing the state transformation $\zeta = (J^T\otimes I_{mn}\hat{\delta})$ with $\zeta = [\zeta_1^T, \ldots, \zeta_M]^T$ and $J^T\mathcal{T}J = \mathrm{diag}\{\tau_i\}$, (38) is further put into

$$\begin{aligned}\dot{V}_c \leq {} & \frac{1}{2}\sum_{i=1}^{M}\zeta_i^T\tau_i[P_cA + A^TP_c - 2c_uq_i\sigma_i(G)P_cBB^TP_c]\zeta_i \\ & - c_u\delta^T(\mathcal{T}\otimes P_cFC)\tilde{S} \\ & - \delta^T(\mathcal{T}\mathbf{1}_M\otimes P_cB)y_r^{\theta}(\theta)\omega\end{aligned}$$

where $\sigma_i(G)$ is the ith eigenvalue of G. Then, one yields that

$$\dot{V}_c \leq -c_4\|\hat{\delta}\|^2 + \sum_{i=1}^{M}c_5\|\hat{\delta}\|\|\tilde{S}_i\| + c_6\|\hat{\delta}\||\omega| \tag{39}$$

where $c_4 = 0.5\min_{i=1,\ldots,M}\tau_i\underline{\sigma}(Q_c)$, $c_5 = c_u\bar{\sigma}(\mathcal{T})\bar{\sigma}(P_cFC)$, and $c_6 = \bar{y}_r^{\theta}\bar{\sigma}(\mathcal{T})\bar{\sigma}(P_c)$.

Since $\|\hat{\delta}\| \geq (2\sum_{i=1}^{M}c_5\|\tilde{S}_i\| + 2c_6|\omega|)/c_4$ makes

$$\dot{V}_c \leq -\frac{1}{2}c_4\|\hat{\delta}\|^2 \tag{40}$$

the subsystem Σ_c governed by (35) is input-to-state stable.

Defining a class $\mathcal{KL}$ function $\beta_c(\cdot)$ and class $\mathcal{K}$ functions $\kappa_{\tilde{S}_i}(\cdot)$ and $\kappa_{\omega}(\cdot)$, it follows that:

$$\|\hat{\delta}(t)\| \leq \beta_c\left(\|\hat{\delta}(0)\|, t\right) + \sum_{i=1}^{M}\kappa_{\tilde{S}_i}\left(\|\tilde{S}_i\|\right) + \kappa_{\omega}(|\omega|) \tag{41}$$

where $\kappa_{\tilde{S}_i}(r) = 2c_5\sqrt{\bar{\sigma}(\mathcal{T}\otimes P_c)}r/c_4\sqrt{\underline{\sigma}(\mathcal{T}\otimes P_c)}$ and $\kappa_{\omega}(r) = 2c_6\sqrt{\bar{\sigma}(\mathcal{T}\otimes P_c)}r/c_4\sqrt{\underline{\sigma}(\mathcal{T}\otimes P_c)}$. ■

IV. Main Results

First, the error dynamics of the interconnection system connected by (13) and (35) is given as follows:

$$\Sigma_{c+l}:\begin{cases}\dot{\hat{\delta}}=(I_M\otimes A-c_u\mathcal{H}\otimes BK)\hat{\delta}\\ \quad-(I_M\otimes FC)\tilde{S}-\rho\\ \quad-(\mathbf{1}_M\otimes B)\left[y_r^{\theta}(\theta)\omega+f_r(\theta,y_r(\theta))\right]\\ \dot{\tilde{\theta}}_a=A_l\tilde{\theta}_a+B_l\hat{\omega}\\ \hat{\omega}=-c_lB_l^TP_l\tilde{\theta}_a+h_\omega\\ h_\omega=-\sum_{i\in\mathcal{N}_l}b_i\rho_l y_r^{\theta T}(\theta)\left(C\hat{e}_i\right).\end{cases}\tag{42}$$

Σ_{c+l} is input-to-state stable, according to the following lemma.

Lemma 7: Consider the interconnection system Σ_{c+l} formed by Σ_c (35) and Σ_l (13) with states being δ, $\tilde{\theta}$, and ω and the input being $\tilde{S}_i$. Σ_{c+l} is input-to-state stable.

Proof: The subsystem Σ_c is proved to be input-to-state stable, according to Lemma 6. Because $|\omega|$ is an element of E_l, (41) is changed into

$$\|\hat{\delta}(t)\|\le\beta_c\left(\|\hat{\delta}(0)\|,t\right)+\sum_{i=1}^{M}\kappa_{\tilde{S}_i}\left(\|\tilde{S}_i\|\right)+\kappa_\omega(\|E_l\|).\tag{43}$$

It follows from Lemma 3 that the subsystem Σ_l is also input-to-state stable. Recalling (19), we have

$$\|E_l(t)\|\le\beta_l(\|E_l(0)\|,t)+\kappa_{\hat{\delta}}\left(\|\hat{\delta}\|\right).\tag{44}$$

It can be observed that the input ω of the subsystem Σ_c is a state of the subsystem Σ_l, and the input $\hat{\delta}$ of the subsystem Σ_l is a state of the subsystem Σ_c. According to Lemma 3, the interconnection system Σ_{c+l} is input-to-state stable when the following condition is satisfied:

$$\kappa_\omega\circ\kappa_\delta(r)=\frac{\rho_l\cdot 4c_2c_6\sqrt{\bar{\sigma}(\Psi_l)}\sqrt{\bar{\sigma}(\mathcal{T}\otimes P_c)}}{c_1c_4\sqrt{\underline{\sigma}(\Psi_l)}\sqrt{\underline{\sigma}(\mathcal{T}\otimes P_c)}}r<r.\tag{45}$$

It follows that:

$$\frac{\rho_l\cdot 4c_2c_6\sqrt{\bar{\sigma}(\Psi_l)}\sqrt{\bar{\sigma}(\mathcal{T}\otimes P_c)}}{c_1c_4\sqrt{\underline{\sigma}(\Psi_l)}\sqrt{\underline{\sigma}(\mathcal{T}\otimes P_c)}}<1.$$

Then, ρ_l is chosen as follows:

$$\rho_l<\frac{c_1c_4\sqrt{\underline{\sigma}(\Psi_l)}\sqrt{\underline{\sigma}(\mathcal{T}\otimes P_c)}}{4c_2c_6\sqrt{\bar{\sigma}(\Psi_l)}\sqrt{\bar{\sigma}(\mathcal{T}\otimes P_c)}}.\tag{46}$$

Letting $E_s=[\|\hat{\delta}\|,\|E_l\|]^T$, E_s satisfies

$$\|E_s(t)\|\le\beta_s(\|E_s(0)\|,t)+\sum_{i=1}^{M}\kappa_{\tilde{S}_i}\left(\|\tilde{S}_i\|\right)\tag{47}$$

where $\beta_s(\cdot)$ is a class $\mathcal{KL}$ function. ■

Finally, the next theorem presents the main result of the proposed method in this article.

Theorem 1: Consider the uncertain MIMO strict-feedback multiagent systems governed by (2) and the parameterized virtual leader governed by (6). If the distributed output-feedback consensus maneuvering controllers are chosen as (22) and (32) and the path update law is chosen as (11), the closed-loop system is input-to-state stable under Assumptions 1 and 2, and all error signals are uniformly bounded.

Proof: The closed-loop system is cascaded by $\Sigma_{o,i}$ and $\Sigma_{o,i}$. The subsystem $\Sigma_{o,i}$ and the subsystem Σ_{c+l} have been proved to be input-to-state stable in Lemmas 5 and 7. Therefore, the resulting closed loop is input-to-state stable by using [52, Lemma 4.6], and then

$$\|E_s(t)\|<\beta_s(\|E_s(0)\|,t)+\sum_{i=1}^{M}\kappa_{\tilde{S}_i}\circ(\kappa_{\varepsilon_i}(\|\varepsilon_i\|)+\kappa_{W_i}(\|W_i\|_{\mathrm{F}})).\tag{48}$$

$\tilde{S}_i$ and $\hat{\delta}$ are uniformly bounded according to Lemma 5 and Lemma 7. Let $\tilde{S}=[\tilde{S}_1^T,\ldots,\tilde{S}_M^T]^T\in\mathbb{R}^{Mmn}$ and $\delta=[\delta_1^T,\ldots,\delta_M^T]^T\in\mathbb{R}^{Mmn}$ with $\delta_i=S_i-Y_r\in\mathbb{R}^{mn}$. Because $\delta=\hat{\delta}-\tilde{S}$, δ is uniformly bounded by

$$\begin{aligned}\lim_{t\to\infty}\|\delta\|&\le\lim_{t\to\infty}\left(\|\hat{\delta}\|+\|\tilde{S}\|\right)\\&\le\lim_{t\to\infty}\left(\|\hat{\delta}\|+\sum_{i=1}^{M}\|\tilde{S}_i\|\right)\\&\le\sum_{i=1}^{M}\left(1+\kappa_{\tilde{S}_i}\right)\circ(\kappa_{\varepsilon_i}(\|\varepsilon_i\|)+\kappa_{W_i}(\|W_i\|_{\mathrm{F}})).\end{aligned}\tag{49}$$

Due to $\|\varepsilon_i\|\le\varepsilon_i^*$ and $\|W_i\|_{\mathrm{F}}\le W_i^*$, (49) is further put into the following form:

$$\lim_{t\to\infty}\|\delta\|\le\sum_{i=1}^{M}\left[2\frac{\sqrt{\bar{\sigma}\left(\Psi_{o,i}\right)}}{c_{i,3}\sqrt{\underline{\sigma}\left(\Psi_{o,i}\right)}}\left(1+\frac{2c_5\sqrt{\bar{\sigma}(\mathcal{T}\otimes P_c)}}{c_4\sqrt{\underline{\sigma}(\mathcal{T}\otimes P_c)}}\right)\times\left(\varepsilon_i^*+\sqrt{\bar{\sigma}(K_{W_i})}W_i^*\right)\right].\tag{50}$$

Define $e=[e_1^T,\ldots,e_M^T]^T$ and $\hat{e}=[\hat{e}_1^T,\ldots,\hat{e}_M^T]^T$. Since $e=\mathcal{H}\delta$ and $\hat{e}=\mathcal{H}\hat{\delta}$, e and $\hat{e}$ can be proved to be uniformly bounded with $\|e\|\le\bar{\sigma}(\mathcal{H})\|\delta\|$ and $\|\hat{e}\|\le\bar{\sigma}(\mathcal{H})\|\hat{\delta}\|$. Considering that the neural network approximation should stay valid at all times, the stability analysis yields a semi-global boundedness result. ■

Remark 5: According to [52, Definition 4.4 and Th. 4.6], (49) shows that for any bounded inputs $\varepsilon_i(t)$ and $W_i(t)$, all error signals in the closed-loop system will remain bounded as t increases. e_i is uniformly bounded and will also converge to a residual set.

Remark 6: The output-feedback consensus maneuvering problem considered herein can also be tackled by alternative methods. For example, when the virtual leader is transformed into the leader model using in [14] and [53], the consensus maneuvering controller can be developed based on a distributed internal model approach proposed in the same references. When system (2) is transformed into a discrete form, necessary and sufficient conditions for consensus maneuvering can be determined by using z-transformation and Routh criterion [54]. In cases where the multiagent system involves additional optimization goals, the proposed method can be combined with a surplus-based accelerated strategy [55].

Remark 7: The proposed method offers several advantages. First, it employs a single control law, simplifying the overall

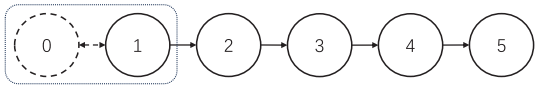

Fig. 1. Relationship among five ASVs.

structure. Second, based on this method, the number of neural networks and adaptation laws can be reduced to just one, simplifying the learning process. Third, the proposed method eliminates the need for additional filters and differentiators. However, a disadvantage of the proposed method is that it requires solving three algebraic Riccati inequalities. On the other hand, adaptive backstepping-like methods [35], [37], [38], [39] have their own advantages. First, by stabilizing each order of the model, the stability analysis of these methods becomes straightforward. Second, these methods do not impose restrictions on the location of unknown parameters or constrain the growth of nonlinearities [56]. Nonetheless, adaptive backstepping-like methods do have disadvantages. First, constructing the $n-1$ virtual control laws and the final control law in a step-by-step manner is necessary. Second, these methods face the inherent challenge of complexity explosion, or additional filters and differentiators must be employed to obtain the derivatives of virtual control laws [39].

Remark 8: The high-order neural observer (22) is constructed based on the structure of the transformed model (3) and (4). The proposed high-order neural observer can also be applied in the adaptive backstepping method. The learning performance of neural networks using these two different methods, based on the same observer, shows no significant difference under the same assumptions and conditions.

V. Simulation Results

A simulation is conducted to demonstrate the performance of the proposed output-feedback consensus maneuvering control method in the distributed formation of ASVs. The formation comprises five ASVs (No. 1–5) and one virtual leader (No. 0), as illustrated in Fig. 1. It should be noted that the desired parameterized path for the virtual leader among the ASV formation is prestored in No. 1 ASV. The dynamics of the ith ASV is expressed as [57]

$$M_i^*\ddot{\eta}_i + C_i^*\dot{\eta}_i + D_i^*\dot{\eta}_i + g_i(\eta_i, \nu_i) = R_i(\psi_i)\tau_i$$

with

$$\begin{cases} M_i^* = R(\psi_i)M_iR^T(\psi_i) \\ C_i^* = R_i(\psi_i)\big[C_i(\nu_i) - M_iR_i^T(\psi_i)\dot{R}_i(\psi_i)\big]R_i^T(\psi_i) \\ D_i^* = R_i(\psi_i)D_i(\nu_i)R_i^T(\psi_i) \end{cases}$$

where $i = 1, \ldots, 5$, $\eta_i = [x_i, y_i, \psi_i]^T \in \mathbb{R}^3$ denotes the output vector in the Earth-fixed coordinate, x_i and y_i mean latitude coordinates and longitude coordinates, respectively, ψ_i is the yaw angle, $\nu_i = [\bar{u}_i, \bar{v}_i, \bar{r}_i]^T \in \mathbb{R}^3$ denotes the velocity vector in the body coordinate, $\bar{u}_i$, $\bar{v}_i$, and $\bar{r}_i$ are surge velocity, sway velocity, and yaw velocity, respectively, $\tau_i \in \mathbb{R}^3$ is the input, $M_i = M_i^T \in \mathbb{R}^{3\times3}$ means the internal matrix related to mass and dimensions, $R_i(\psi_i) \in \mathbb{R}^{3\times3}$ represents the rotation matrix with $R_i^{-1}(\psi_i) = R_i^T(\psi_i)$, $C_i(\nu_i) \in \mathbb{R}^{3\times3}$ means the skew-symmetric Coriolis and centripetal terms matrix, $D_i(\nu_i) \in \mathbb{R}^{3\times3}$ means the damping term, $g_i(\eta_i, \nu_i) \in \mathbb{R}^3$ means the unknown hydrodynamics, and $w_i \in \mathbb{R}^3$ means the ocean disturbances simulated by the white Gaussian noise herein. Fossen [57] provided internal parameters of the ASV.

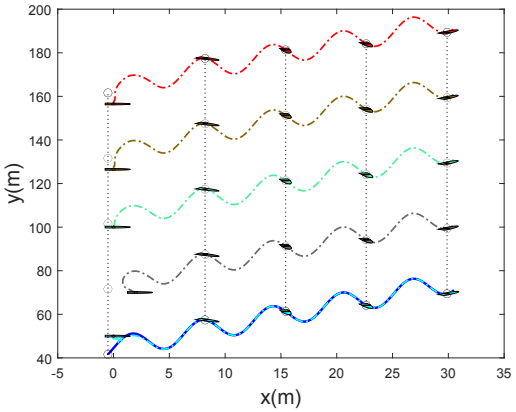

Fig. 2. Output trajectories of five ASVs.

Furthermore, we can transform the original model of ASVs into the form like (3). The new model is

$$\begin{cases} \dot{x}_{i,1} = x_{i,2} \\ \dot{x}_{i,2} = u_i + f_i\big(x_{i,1}, x_{i,2}\big) + w_i \\ y_i = x_{i,1} \end{cases}$$

where $x_{i,1} = \eta_i$, $x_{i,2} = \dot{\eta}_i$, $u_i = (M_i^*)^{-1}R_i(\psi_i)\tau_i$, and $f_i(x_{i,1}, x_{i,2}) = (M_i^*)^{-1}[-C_i^*x_{i,2} - D_i^*x_{i,2} + g_i(\eta_i, \nu_i)]$.

The virtual leader is steered along a parameterized path $y_r(\theta) = [\theta+0.5, 5\sin(\theta+0.5)+45+\theta, \arctan(5\cos(\theta+0.5)+1)]^T$, and the given dynamic specification is $\bar{\theta}_{\text{ref}} = [0.3t, 0.3]^T$. The control parameters are set to

$$K = \begin{bmatrix} 2.2361 & 0 & 0 & 3.0777 & 0 & 0 \\ 0 & 2.2361 & 0 & 0 & 3.0777 & 0 \\ 0 & 0 & 2.2361 & 0 & 0 & 3.0777 \end{bmatrix}$$

$$F = \begin{bmatrix} 60 & 0 & 0 \\ 0 & 60 & 0 \\ 0 & 0 & 60 \\ 1200 & 0 & 0 \\ 0 & 1200 & 0 \\ 0 & 0 & 1200 \end{bmatrix}$$

$c = 30$, $h_i = 1$, $\Gamma_i = \text{diag}\{3000, 3000, 3000\}$, $K_{W_i} = \text{diag}\{0.00001, 0.00001, 0.00001\}$, $\Gamma_{i,fr} = 50$, $k_{i,fr} = 0.0001$, $\lambda_l = 5$, $\rho_l = 1$. To avoid collisions, the estimated consensus maneuvering error is redefined as $\hat{e}_i = \sum_{j\in\mathcal{F}_i} a_{i,j}(\hat{S}_i - \hat{S}_j - d_i) + a_{i,r}(\hat{S}_i - Y_r - d_0)$, where $d_i, d_0 \in \mathbb{R}^{mn}$ denote the desired formation distances.

Simulation results are presented in the following figures. Output trajectories of five ASVs are displayed in Fig. 2, demonstrating the convergence of follower trajectories to a desired formation guided by the parameterized path in 2-D space, thus implementing the consensus maneuvering formation. The curve of the path variable θ is depicted in Fig. 3, illustrating the update of the path variable according to the given specification. Figs. 4 and 5 showcase the observational effect of the proposed high-order neural observer, implying

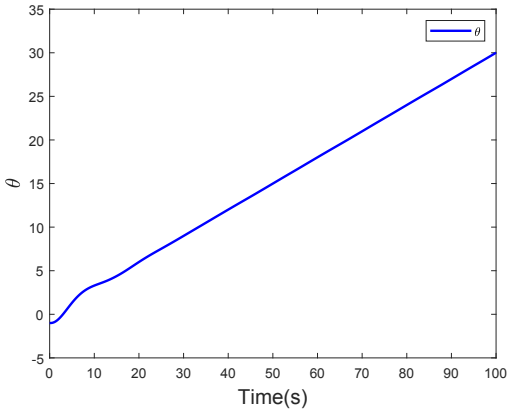

Fig. 3. Evolution of the path variable.

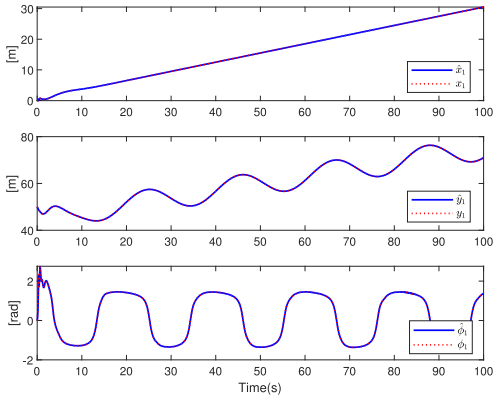

Fig. 4. Output observation using the proposed high-order neural observer.

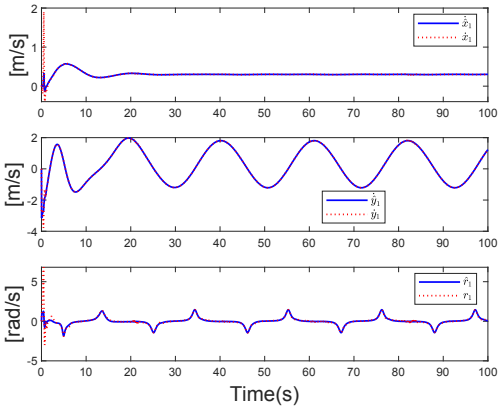

Fig. 5. Velocity observation using the proposed high-order neural observer.

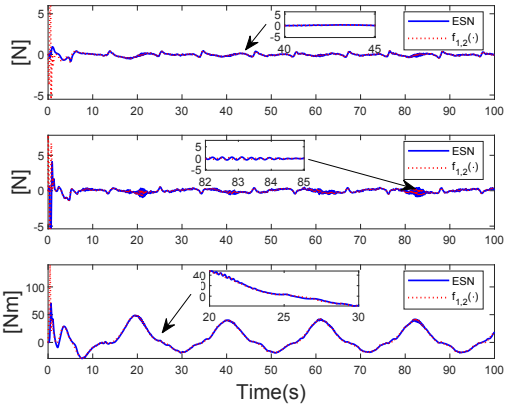

Fig. 6. Learning profiles of the ESN.

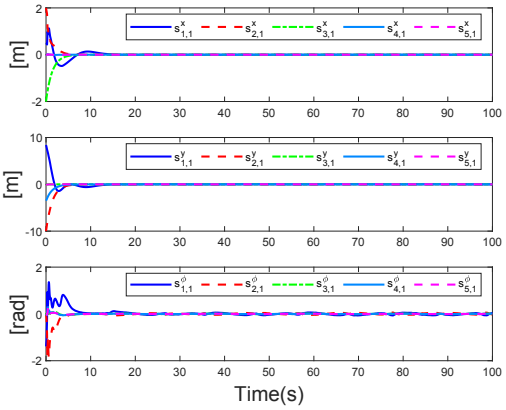

Fig. 7. Output errors using the proposed control method.

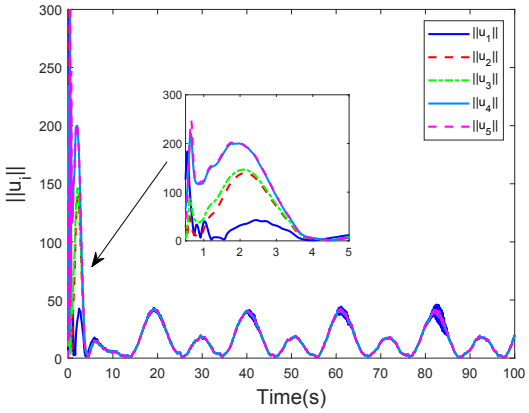

Fig. 8. Control inputs using the proposed control method.

accurate state observation based on the output information of ASVs. The approximation performance of the echo state network is portrayed in Fig. 6, revealing that internal uncertainties can be effectively approximated by the proposed method. The evolution of output errors using the proposed output-feedback consensus maneuvering control method is presented in Fig. 7, indicating that the output errors of all ASVs converge to a small neighborhood of the origin. Fig. 8 illustrates the norm of inputs for all ASVs using the proposed method.

To further validate the proposed high-order neural observer, an additional step disturbance is introduced at $t = 50$ s. All other conditions, including agent dynamics, the virtual leader, communication topology, and parameters, remain the same. Fig. 9 depicts the learning profile of the echo state network, while Fig. 10 illustrates the observation performance of the proposed high-order neural observer. Together, Figs. 9 and 10 show that the proposed high-order neural observer exhibits good transient performance.

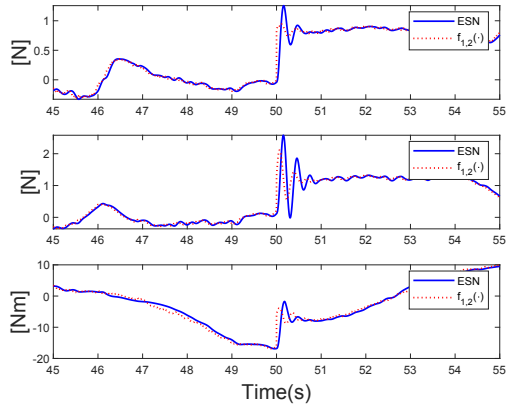

Fig. 9. Learning profiles of the ESN during step disturbance.

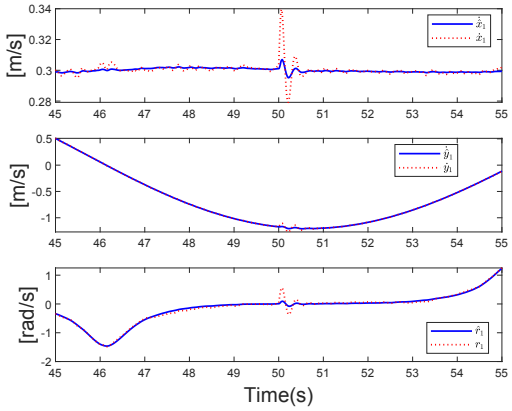

Fig. 10. Velocity observation using the proposed high-order neural observer during step disturbance.

VI. Conclusion

This article investigates distributed output-feedback consensus maneuvering for uncertain MIMO strict-feedback multiagent systems. The proposed distributed neural observer-based adaptive consensus maneuvering control method is distinguished from the backstepping-like observer-based consensus control methods, which typically involve multiple control laws and approximators. In contrast, the proposed method employs only one control law and one approximator, irrespective of the system's order, leading to a reduction in the number of control parameters. Furthermore, unlike existing maneuvering control methods based on state-feedback design, which primarily address second-order dynamic tasks, the proposed method does not necessitate full-state information and is applicable to *n*th-order dynamic tasks. The overall output-feedback consensus maneuvering closed-loop is proven to be input-to-state stable through interconnected and cascade systems analysis. In future work, practical constraints, such as switching typologies, actuator saturation, and time delays, will be considered. Besides, we will try to speed up the convergence speed, which finite-time consensus maneuvering and fixed-time consensus maneuvering are further investigated.

References

[1] H. Ishii, Y. Wang, and S. Feng, "An overview on multi-agent consensus under adversarial attacks," *Annu. Rev. Control*, vol. 53, pp. 252–272, May 2022.

[2] P. Shi and B. Yan, "A survey on intelligent control for multiagent systems," *IEEE Trans. Syst., Man, Cybern., Syst.*, vol. 51, no. 1, pp. 161–175, Jan. 2021.

[3] Y. Tang, D. Zhang, P. Shi, W. Zhang, and F. Qian, "Event-based formation control for nonlinear multiagent systems under DoS attacks," *IEEE Trans. Autom. Control*, vol. 66, no. 1, pp. 452–459, Jan. 2021.

[4] A. Jadbabaie, J. Lin, and A. Morse, "Coordination of groups of mobile autonomous agents using nearest neighbor rules," *IEEE Trans. Autom. Control*, vol. 48, no. 6, pp. 988–1001, Jun. 2003.

[5] Y.-Y. Qian, L. Liu, and G. Feng, "Output consensus of heterogeneous linear multi-agent systems with adaptive event-triggered control," *IEEE Trans. Autom. Control*, vol. 64, no. 6, pp. 2606–2613, Jun. 2019.

[6] N. Jin, J. Xu, and H. Zhang, "Distributed optimal consensus control of multiagent systems involving state and control dependent multiplicative noise," *IEEE Trans. Autom. Control*, vol. 68, no. 12, pp. 7787–7794, Dec. 2023, doi: 10.1109/TAC.2023.3246422.

[7] Z. Li, G. Wen, Z. Duan, and W. Ren, "Designing fully distributed consensus protocols for linear multi-agent systems with directed graphs," *IEEE Trans. Autom. Control*, vol. 60, no. 4, pp. 1152–1157, Apr. 2015.

[8] H. Jiang and H. Zhang, "Output sign-consensus of heterogeneous multiagent systems over fixed and switching signed graphs," *Int. J. Robust Nonlin. Control*, vol. 30, no. 5, pp. 1938–1955, 2020.

[9] Z. Sun, H. Zhang, and F. L. Lewis, "Output sign-consensus of heterogeneous multiagent systems over fixed and switching signed graphs: An observer-based approach," *Int. J. Robust Nonlin. Control*, vol. 31, no. 12, pp. 5849–5864, 2021.

[10] B. Cheng and Z. Li, "Coordinated tracking control with asynchronous edge-based event-triggered communications," *IEEE Trans. Autom. Control*, vol. 64, no. 10, pp. 4321–4328, Oct. 2019.

[11] W. Liu and J. Huang, "Leader-following consensus for linear multiagent systems via asynchronous sampled-data control," *IEEE Trans. Autom. Control*, vol. 65, no. 7, pp. 3215–3222, Jul. 2020.

[12] W. He and Z. Mo, "Secure event-triggered consensus control of linear multiagent systems subject to sequential scaling attacks," *IEEE Trans. Cybern.*, vol. 52, no. 10, pp. 10314–10327, Oct. 2022.

[13] D. Wang, Z. Wang, and C. Wen, "Distributed optimal consensus control for a class of uncertain nonlinear multiagent networks with disturbance rejection using adaptive technique," *IEEE Trans. Syst., Man, Cybern., Syst.*, vol. 51, no. 7, pp. 4389–4399, Jul. 2021.

[14] M. Lu and L. Liu, "Consensus of heterogeneous second-order nonlinear uncertain multiagent systems under switching networks," *IEEE Trans. Autom. Control*, vol. 66, no. 7, pp. 3331–3338, Jul. 2021.

[15] Y. H. Choi and S. J. Yoo, "Distributed quantized feedback design strategy for adaptive consensus tracking of uncertain strict-feedback nonlinear multiagent systems with state quantizers," *IEEE Trans. Cybern.*, vol. 52, no. 7, pp. 7069–7083, Jul. 2022.

[16] H. Du, G. Wen, D. Wu, Y. Cheng, and J. Lü, "Distributed fixed-time consensus for nonlinear heterogeneous multi-agent systems," *Automatica*, vol. 113, Mar. 2020, Art. no. 108797.

[17] Y. Sun, B. Yan, P. Shi, and C.-C. Lim, "Consensus for multiagent systems under output constraints and unknown control directions," *IEEE Syst. J.*, vol. 17, no. 1, pp. 1035–1044, Mar. 2023.

[18] D. B. Dačić and P. V. Kokotović, "Path-following for linear systems with unstable zero dynamics," *Automatica*, vol. 42, no. 10, pp. 1673–1683, 2006.

[19] D. B. Dacic, M. V. Subbotin, and P. V. Kokotovic, "Control effort reduction in tracking feedback laws," *IEEE Trans. Autom. Control*, vol. 51, no. 11, pp. 1831–1837, Nov. 2006.

[20] R. Skjetne, T. I. Fossen, and P. V. Kokotović, "Robust output maneuvering for a class of nonlinear systems," *Automatica*, vol. 40, no. 3, pp. 373–383, Mar. 2004.

[21] Y. Zhang, D. Wang, and Z. Peng, "Consensus maneuvering for a class of nonlinear multivehicle systems in strict-feedback form," *IEEE Trans. Cybern.*, vol. 49, no. 5, pp. 1759–1767, May 2019.

[22] Y. Zhang, D. Wang, Z. Peng, and T. Li, "Distributed containment maneuvering of uncertain multiagent systems in MIMO strict-feedback form," *IEEE Trans. Syst., Man, Cybern., Syst.*, vol. 51, no. 2, pp. 1354–1364, Feb. 2021.

[23] J. Cenerini, M. W. Mehrez, J. Woo Han, S. Jeon, and W. Melek, "Model predictive path following control without terminal constraints for holonomic mobile robots," *Control Eng. Pract.*, vol. 132, Mar. 2023, Art. no. 105406.

[24] N. Gu, D. Wang, Z. Peng, and J. Wang, "Safety-critical containment maneuvering of underactuated autonomous surface vehicles based on neurodynamic optimization with control barrier functions," *IEEE Trans. Neural Netw. Learn. Syst.*, vol. 34, no. 6, pp. 2882–2895, Jun. 2023.

[25] G. Lv, Z. Peng, Y. Li, L. Liu, and D. Wang, "Barrier-certified model predictive cooperative path following control of connected autonomous surface vehicles," *IEEE Trans. Netw. Sci. Eng.*, vol. 10, no. 6, pp. 3354–3367, Dec. 2023.

[26] Y. Yan, S. Yu, X. Gao, D. Wu, and T. Li, "Continuous and periodic event-triggered sliding-mode control for path following of underactuated surface vehicles," *IEEE Trans. Cybern.*, vol. 54, no. 1, pp. 449–461, Jan. 2024, doi: 10.1109/TCYB.2023.3265039.

[27] L. Liu, D. Wang, Z. Peng, and Q.-L. Han, "Distributed path following of multiple under-actuated autonomous surface vehicles based on data-driven neural predictors via integral concurrent learning," *IEEE Trans. Neural Netw. Learn. Syst.*, vol. 32, no. 12, pp. 5334–5344, Dec. 2021.

[28] Z. Peng, Y. Jiang, L. Liu, and Y. Shi, "Path-guided model-free flocking control of unmanned surface vehicles based on concurrent learning extended state observers," *IEEE Trans. Syst., Man, Cybern., Syst.*, vol. 53, no. 8, pp. 4729–4739, Aug. 2023.

[29] J. Zhang, X. Xiang, W. Li, and Q. Zhang, "Adaptive saturated path following control of underactuated AUV with unmodeled dynamics and unknown actuator hysteresis," *IEEE Trans. Syst., Man, Cybern., Syst.*, vol. 53, no. 10, pp. 6018–6030, Oct. 2023.

[30] W. Xie, D. Cabecinhas, R. Cunha, and C. Silvestre, "Cooperative path following control of multiple quadcopters with unknown external disturbances," *IEEE Trans. Syst., Man, Cybern., Syst.*, vol. 52, no. 1, pp. 667–679, Jan. 2022.

[31] H. Li, W. Li, and J. Gu, "Distributed output tracking control of nonlinear multi-agent systems with unknown time-varying powers," *Int. J. Control*, vol. 95, no. 11, pp. 2960–2971, 2022.

[32] J. Zhou, Y. Lv, G. Wen, and X. Yu, "Resilient consensus of multiagent systems under malicious attacks: Appointed-time observer-based approach," *IEEE Trans. Cybern.*, vol. 52, no. 10, pp. 10187–10199, Oct. 2022.

[33] Y. Dong and J. Chen, "Nonlinear observer-based approach for cooperative control of networked rigid spacecraft systems," *Automatica*, vol. 128, Jun. 2021, Art. no. 109552.

[34] W. Li, L. Liu, and G. Feng, "Distributed output-feedback tracking of multiple nonlinear systems with unmeasurable states," *IEEE Trans. Syst., Man, Cybern., Syst.*, vol. 51, no. 1, pp. 477–486, Jan. 2021.

[35] W. Wu, Y. Li, and S. Tong, "Neural network output-feedback consensus fault-tolerant control for nonlinear multiagent systems with intermittent actuator faults," *IEEE Trans. Neural Netw. Learn. Syst.*, vol. 34, no. 8, pp. 4728–4740, Aug. 2023.

[36] L. Zhang, W.-W. Che, B. Chen, and C. Lin, "Adaptive fuzzy output-feedback consensus tracking control of nonlinear multiagent systems in prescribed performance," *IEEE Trans. Cybern.*, vol. 53, no. 3, pp. 1932–1943, Mar. 2023.

[37] W. Wang and S. Tong, "Observer-based adaptive fuzzy containment control for multiple uncertain nonlinear systems," *IEEE Trans. Fuzzy Syst.*, vol. 27, no. 11, pp. 2079–2089, Nov. 2019.

[38] W. Wang, Y. Li, and S. Tong, "Neural-network-based adaptive event-triggered consensus control of nonstrict-feedback nonlinear systems," *IEEE Trans. Neural Netw. Learn. Syst.*, vol. 32, no. 4, pp. 1750–1764, Apr. 2021.

[39] Z. Peng, L. Liu, and J. Wang, "Output-feedback flocking control of multiple autonomous surface vehicles based on data-driven adaptive extended state observers," *IEEE Trans. Cybern.*, vol. 51, no. 9, pp. 4611–4622, Sep. 2021.

[40] F. Lewis, H. Zhang, K. Hengster-Movric, and A. Das, *Cooperative Control of Multi-Agent Systems: Optimal and Adaptive Design Approaches* (Communications and Control Engineering). London, U.K.: Springer-Verlag, 2014.

[41] H. Zhang and F. L. Lewis, "Adaptive cooperative tracking control of higher-order nonlinear systems with unknown dynamics," *Automatica*, vol. 48, no. 7, pp. 1432–1439, 2012.

[42] J.-H. Park, S.-H. Kim, and T.-S. Park, "Output-feedback adaptive neural controller for uncertain pure-feedback nonlinear systems using a high-order sliding mode observer," *IEEE Trans. Neural Netw. Learn. Syst.*, vol. 30, no. 5, pp. 1596–1601, May 2019.

[43] R. Wang, F.-S. Yu, Y.-J. Liu, J.-Y. Wang, L. Yu, and L. Yun Zhao, "A novel adaptive non-backstepping VUFC algorithm for a class of MIMO nonlinear systems with unknown dead-zones in pure-feedback form," *Nonlin. Anal., Hybrid Syst.*, vol. 31, pp. 200–219, Feb. 2019.

[44] T. Faulwasser, T. Weber, P. Zometa, and R. Findeisen, "Implementation of nonlinear model predictive path-following control for an industrial robot," *IEEE Trans. Control Syst. Technol.*, vol. 25, no. 4, pp. 1505–1511, Jul. 2017.

[45] Z.-P. Jiang, A. R. Teel, and L. Praly, "Small-gain theorem for ISS systems and applications," *Math. Control, Signals Syst.*, vol. 7, no. 2, pp. 95–120, 1994.

[46] Y. Pan and J. Wang, "Model predictive control of unknown nonlinear dynamical systems based on recurrent neural networks," *IEEE Trans. Ind. Electron.*, vol. 59, no. 8, pp. 3089–3101, Aug. 2012.

[47] R. A. Horn and C. R. Johnson, *Matrix Analysis*. Cambridge, U.K.: Cambridge Univ. Press, 2012.

[48] X. Zhao, X. Wang, S. Zhang, and G. Zong, "Adaptive neural Backstepping control design for a class of nonsmooth nonlinear systems," *IEEE Trans. Syst., Man, Cybern., Syst.*, vol. 49, no. 9, pp. 1820–1831, Sep. 2019.

[49] C. Kwan and F. Lewis, "Robust backstepping control of nonlinear systems using neural networks," *IEEE Trans. Syst., Man, Cybern. Part-A, Syst. Humans*, vol. 30, no. 6, pp. 753–766, Nov. 2000.

[50] S. Sastry and A. Isidori, "Adaptive control of linearizable systems," *IEEE Trans. Autom. Control*, vol. 34, no. 11, pp. 1123–1131, Nov. 1989.

[51] C. Schwartz and I. Mareels, "Comments on "adaptive control of linearizable systems" by S.S. Sastry and A. Isidori," *IEEE Trans. Autom. Control*, vol. 37, no. 5, pp. 698–701, May 1992.

[52] H. K. Khalil, *Nonlinear Control*. Boston, MA, USA: Pearson, 2014.

[53] M. Lu and L. Liu, "Robust Synchronization control of switched networked euler–lagrange systems," *IEEE Trans. Cybern.*, vol. 52, no. 7, pp. 6834–6842, Jul. 2022.

[54] D. Wang, D. Wang, and W. Wang, "Necessary and sufficient conditions for containment control of multi-agent systems with time delay," *Automatica*, vol. 103, pp. 418–423, May 2019.

[55] D. Wang, Z. Wang, J. Lian, and W. Wang, "Surplus-based accelerated algorithms for distributed optimization over directed networks," *Automatica*, vol. 146, Dec. 2022, Art. no. 110569.

[56] I. Kanellakopoulos, P. V. Kokotovic, and A. S. Morse, "Systematic design of adaptive controllers for feedback linearizable systems," in *Proc. Am. Control Conf.*, 1991, pp. 649–654.

[57] T. I. Fossen, *Handbook of Marine Craft Hydrodynamics and Motion Control*, Hoboken, NJ, USA: Wiley, Inc., 2011.

Yibo Zhang (Member, IEEE) received the B.E. degree in marine electronic and electrical engineering and the Ph.D. degree in marine electrical engineering from Dalian Maritime University, Dalian, China, in 2014 and 2021, respectively.

He is a Postdoctoral Fellow with the Department of Automation, Shanghai Jiao Tong University, Shanghai, China. His current research interests include cooperative control and intelligent control of multiagent systems and marine vehicles.

Wentao Wu (Graduate Student Member, IEEE) received the M.E. degree in electrical engineering from Dalian Maritime University, Dalian, China, in 2021. He is currently pursuing the Ph.D. degree in electronic information with Shanghai Jiao Tong University, Shanghai, China.

His current research interests include unmanned surface vehicles, formation control, adaptive control, and safety control.

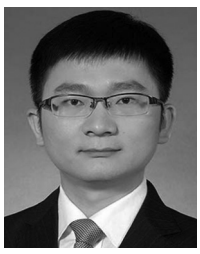

Weixing Chen received the B.S. degree from the China University of Mining and Technology, Xuzhou, China, in 2011, and the Ph.D. degree from Shanghai Jiao Tong University, Shanghai, China, in 2016.

He is currently an Associate Professor with the School of Mechanical Engineering, Shanghai Jiao Tong University. His research interests include wave energy converter and ocean robot.

Haibo Lu received the B.Eng. degree in mechanical engineering from Central South University, Changsha, Hunan, China, in 2011, and the Ph.D. degree in mechanical engineering from The University of Queensland, Brisbane, QLD, Australia, in 2017.

He is currently a Research Assistant Professor with the Robotics Research Center, Peng Cheng Laboratory, Shenzhen, China. From 2018 to 2019, he was a Lecturer with the School of Traffic and Transportation Engineering, Central South University. His current research interests include model predictive control, multirobot systems, ocean robotics, and cooperative control.

Weidong Zhang (Senior Member, IEEE) received the B.S., M.S., and Ph.D. degrees from Zhejiang University, Hangzhou, China, in 1990, 1993, and 1996, respectively,

Then, he worked as a Postdoctoral Fellow with Shanghai Jiao Tong University, Shanghai, China. He joined Shanghai Jiao Tong University in 1998 as an Associate Professor and has been a Full Professor since 1999. From 2003 to 2004, he worked with the University of Stuttgart, Stuttgart, Germany, as an Alexander von Humboldt Fellow. He is currently the Director of the Engineering Research Center of Marine Automation, Shanghai Municipal Education Commission, and the Director of the Marine Intelligent System Engineering Research Center, Ministry of Education, China. He is the author of 265 SCI papers and one book, and holds 72 patents. His research interests include control theory, machine learning theory, and their applications in industry and autonomous systems.

Prof. Zhang is a recipient of the National Science Fund for Distinguished Young Scholars, China, and a Cheung Kong Scholar, Ministry of Education, China.